Redox Signaling in an *In Vivo* Murine Model of Low Magnitude Oscillatory Wall Shear Stress

Nick J. Willett,[1,3] Kousik Kundu,[1,3] Sarah F. Knight,[2] Sergey Dikalov,[2] Niren Murthy,[1,3] and W. Robert Taylor[1–4]

Abstract

Wall Shear Stress (WSS) has been identified as an important factor in the pathogenesis of atherosclerosis. We utilized a novel murine aortic coarctation model to acutely create a region of low magnitude oscillatory WSS *in vivo*. We employed this model to test the hypothesis that acute changes in WSS *in vivo* induce upregulation of inflammatory proteins, mediated by reactive oxygen species (ROS). Superoxide generation and VCAM-1 expression both increased in regions of low magnitude oscillatory WSS. WSS-dependent superoxide formation was attenuated by tempol treatment, but was unchanged in p47 *phox* knockout (ko) mice. However, in both the p47 phox ko mice and the tempol-treated mice, low magnitude oscillatory WSS produced an increase in VCAM-1 expression comparable to control mice. Additionally, this same VCAM-1 expression was observed in ebselen-treated mice and catalase overexpressing mice. These results suggest that although the redox state is important to the overall pathogenesis of atherosclerosis, the initial WSS-dependent inflammatory response leading to lesion localization is not dependent on ROS. *Antioxid. Redox Signal.* 15, 1369–1378.

Introduction

Mechanisms of shear-dependent Atherogenesis

ATHEROSCLEROSIS is an inflammatory cardiovascular disease that is localized to specific regions of the vasculature. These regions are uniquely characterized by disturbed flow that is commonly associated with low magnitude oscillatory wall shear stress (LO WSS). Reactive oxygen species (ROS) have been implicated as important mediators in the flow-dependent localization of atherosclerotic lesion formation.

Studies have demonstrated that oxidative stress increases in endothelial cells after exposure to LO WSS. Primary contributors to the endothelial oxidative state are the NADPH oxidase enzymes, which are regulated in response to different flow patterns. LO WSS increases the expression of Nox 1, Nox 2, and Nox 4 (15, 33). Consistent with that finding, superoxide levels increase *in vitro* after endothelial cells are acutely exposed LO WSS (15, 16, 21, 32, 33). This shear-dependent superoxide generation is attenuated in cells from p47 *phox* knockout (ko) mice, or by treatment with either siNox1 or 2-DOG, an inhibitor of the pentose shunt pathway for NADPH production (15, 16, 33). Supporting the *in vitro* data, *in vivo* studies have also shown that acute induction of LO WSS in a partial carotid ligation model induces atherosclerotic lesion

formation, which can be attenuated in p47 phox ko mice. These data together suggest that superoxide is generated in response to LO WSS through an NADPH oxidase mechanism, and in particular implicate the involvement of Nox 2. Additional studies have implicated this increase in ROS levels as a critical mechanotransduction signaling event leading to initiation of an inflammatory response and atherosclerotic lesion development.

One of the earliest identifiable mechanisms involved in atherogenesis is the increased expression of cellular adhesion molecules which then mediate the infiltration of leukocytes into the vessel wall. Cellular adhesion molecules, particularly vascular cell adhesion molecule (VCAM)-1, have been shown to be responsive to WSS, implicating them as a critical mediator in the localization of plaque formation. While there is general agreement that VCAM-1 is upregulated by LO WSS, some *in vitro* studies have reported differing data (4, 5, 23, 24, 33). Additionally, there is evidence that antioxidant treatment can attenuate increased expression of VCAM-1, suggesting that ROS mediate VCAM-1 expression in response to LO WSS (3, 23, 28). The varying cell types (MAECS, HUVECS, or BAECS), time courses (6 hours to 24 hours), flow environments, culture conditions, and environmental factors *in vitro* make an *in vivo* study essential for determining the molecular mechanisms that mediate shear induced expression of cell adhesion molecules.

[1]The Wallace H. Coulter Department of Biomedical Engineering and [2]Department of Medicine, Division of Cardiology, Emory University School of Medicine, Atlanta, Georgia.
[3]Georgia Institute of Technology, Atlanta, Georgia.
[4]Atlanta VA Medical Center, Atlanta, Georgia.

In vivo studies have shown that VCAM-1 expression increases in regions of LO WSS (6, 7, 17, 25, 35). These findings are particularly relevant in lesion formation, as studies using VCAM-1-deficient mice have revealed attenuated lesion formation in regions of disturbed flow (7). Though VCAM-1 ko is embryonic lethal, these mice are VCAM-1 domain 4-deficient (D4D) and have decreased VCAM-1 expression. Interestingly, ko mouse models of other adhesion molecules, such as ICAM-1, do not have attenuated lesion formation in areas of disturbed flow (7).

These data led us to hypothesize that in an *in vivo* model of LO WSS, superoxide levels would increase in an NADPH oxidase-dependent manner and that this increase in superoxide would then mediate shear-dependent VCAM-1 expression.

Our primary objective in this study was to develop a new *en face* technique using a novel superoxide sensitive dye, hydro-Cy3, to characterize endothelial superoxide levels in aortic regions with differing WSS profiles (19). We used a combination of transgenic animal models and reagent treatments to investigate the specificity of the dye and the source of endothelial superoxide. Our secondary objective was to investigate whether superoxide mediates the increase in VCAM-1 expression observed in regions of LO WSS. This study will provide insight into the early mechanisms leading to atherosclerotic lesion localization and possibly present novel therapeutic targets for the prevention of atherosclerosis.

Materials and Methods

Animals

Male C57BL/6 mice were purchased from Jackson Laboratories, (Bar Harbor, Maine). P47 phox $^{-/-}$ mice and the corresponding C57BL/6 controls were purchased from Taconic Farms, Inc. (Hudson, NY). Catalase-overexpressing mice were bred in house in the Department of Animal Resources at Emory University. These mice have increased expression of human catalase in vascular tissue through the endothelial specific, Tie-2, promoter. Tempol (4-Hydroxy-TEMPO, Sigma Aldrich, St. Louis, MO) was administered in drinking water at a concentration of 1 mM, a commonly used dose (31, 37). Tempol was administered intravenously by osmotic mini-pump at a rate of $40*10^{-6}$ mol/kg/min. This was the same concentration (100 mM) previously used for osmotic mini-pumps, but using a pump with an increased pumping rate of 9.89 μl/h (10, 18, 37). Both modes of administration were performed with a one-day pretreatment, before surgery, and then continued for the 72 h time course (total of 4 days treatment). Ebselen (Sigma Aldrich) was administered by osmotic mini-pump subcutaneously at a rate of 10 mg/kg/day. To get Ebselen into solution, it was first dissolved in DMSO which was then mixed with saline to a final concentration of 50% DMSO by volume. Control mice were given mini-pumps with 50% DMSO by volume, the same DMSO concentration used for the ebselen treatment group. Male mice aged 11–13 weeks were used for this study. The animals were housed and cared for according to the guidelines approved by the Emory University Institutional Animal Care and Use Committee.

Osmotic mini-pump implantation

Mice were anesthetized using isoflurane (oxygen delivered at 0.5 l/min with 3% isoflurane for induction and 1.5% iso-flurane for maintenance). For tempol pumps, fur was removed using a dilapatory (Nair) and an incision was made in the neck to expose the jugular vein. A jugular catheter attached to a primed mini-osmotic pump (Alzet osmotic mini-pump 2ML1, Durect Corporation, Cupertino, CA) was inserted and tied into the jugular vein and the pump inserted subcutaneously at the back of the neck. The neck wound was closed using sutures, and mice were administered buprenorphine as needed. For ebselen pumps, the fur was removed from the back, a small incision was made, and the pump (Alzet osmotic mini-pump 1007D) was implanted subcutaneously.

Coarctation surgery

Mice were anesthesized using isoflurane as described above. All hair was removed from the surgical field by first shaving using clippers, then applying a depilatory (Nair). The skin was then sterilized using betadine, and an incision was made through the skin and peritoneum of the abdomen. The abdominal cavity was exposed using a self-retaining retractor. The intestines were displaced from the abdominal cavity and placed between two sterile pledglets of gauze soaked in saline. The abdominal aorta was then located using a dissecting microscope (SZ61, Olympus). Periadventitial fat was removed by performing a blunt dissection with micro-forceps. The nitinol clip was then deformed to an open state and placed underneath the aorta. The body temperature from the mouse thermally activated the recovery response of the niti-nol clip, inducing a defined degree of coarctation of the aorta. The intestines were then returned to the abdominal cavity and the peritoneum and skin was sewn together with absorbable sutures. Finally, surgical staples were applied along the incision line to ensure proper healing. The animals were then kept on heating pads during recovery and given buprenorphine (0.01 mg/kg intraperitoneal) as necessary.

Computational fluid dynamics

A representative computational fluid dynamic model was generated. Detailed methods for the process were published previously (unpublished observation in review). Briefly, inlet velocity conditions were obtained using MR velocimetry (2). The suprarenal region of the aorta was located and cine images were acquired taking ten frames, equally spaced over the cardiac cycle. Morphologic boundary conditions were obtained using uCT, as described previously (11, 35). Abdominal aortic morphology was then imported into Geomagic software (Geomagic Inc., Research Triangle Park, NC). Files were processed *in silico* and exported to GAMBIT (Ansys, Canonsburg, PA) where mesh and boundary layers were applied. The files were exported as .mesh and imported into FLUENT (Ansys). Blunt, cross-sectional averaged, inlet velocity profiles over the time course of a cardiac cycle were obtained from MR phase contrast velocimetry. Outlet conditions were set to 80 mmHg as an approximate mean arterial pressure. Maps of WSS were then generated in Fluent (Kitware, Inc, Clifton Park, NY).

Hydro-Cy3 staining

Animals were euthanized using CO_2 inhalation. The thoracic cavity was opened and the inferior vena cava was cut. A

needle was placed in the left ventricle and the vasculature was perfused at a pressure of 100 mmHg with 0.9% normal saline for 5 minutes. The perfusion was continued with a hydro-Cy3 dilution (stock solution: 2 mg hydro-Cy3 dissolved in 2 ml methanol, working solution: 500 μl stock solution in 100 ml 0.9% normal saline) for 5 min. This was followed by pressure perfusion with 10% neutral buffered formalin for 5 min and then a rinse with normal saline. Aortas were excised and washed in phosphate-buffered saline (PBS). Samples were then mounted *en face* on glass slides using Vectashield with DAPI (Vector Labs, Burlingame, CA).

En Face *quantum dot immunohistochemistry*

Tissues were prepared in accordance with previously described methods (12). Animals were euthanized using CO_2 inhalation. The thoracic cavity was opened and a needle was placed in the left ventricle. The vasculature was perfused at a pressure of 100 mmHg with 0.9% normal saline for 5 min, followed by 10% neutral buffered formalin for 5 min and then rinsed again with saline. Aortas were excised, then washed in PBS, before being permeabilized in 0.2% Triton X-100 (Sigma Aldrich). Aortas were then washed overnight in a humid chamber at 4°C with anti-VCAM1 antibody diluted at 1:100 in blocking buffer (PBS, 2% BSA, 5% goat serum). The following morning, aortas were rinsed with PBS, then washed with secondary antibodies conjugated to 655 quantum dots (Invitrogen, Carlsbad, CA) at a dilution of 1:100 in blocking buffer (PBS, 2% BSA). Quantum dots do not penetrate into the media and therefore the staining is endothelial specific (12). Aortas were then mounted *en face* on glass slides using Vectashield with DAPI (Vector Labs).

Microscopy and quantification of fluorescence intensity

Procedures were described previously (12). *En face* images were collected using a Zeiss LSM 510 META single-photon microscope with a 63x (Plan-Neofluor, NA 1.3) oil immersion objective connected to an inverted Zeiss Axiovert 100 microscope. Separation of the emission signals was performed using the META detector with a 40 nm window for samples stained with quantum dots and a long pass filter for samples stained with the hydro-Cy3. Region of interest was determined using an external registration with a notched slide. Three replicate images from each region of interest were obtained. Fluorescence intensity and percent surface area were quantified using the frequency histogram function of the LSM-510 examiner software.

Electron spin resonance

Plasma tempol concentrations were quantified by electron spin resonance spectrometry. Mouse plasma samples were separated from whole blood by centrifugation and then stored at −80°C. Thawed plasma samples were taken up into a glass capillary tube and placed into a Bruker EMX electron spin resonance spectrometer. Tempol produces a characteristic 3-peak spectra and the concentration of tempol is relative to peak intensity. Therefore, tempol concentration was quantified by measuring the intensity of the first peak. A standard curve was produced by measuring the intensity of the peak from standard tempol concentrations. Intensity measurements were then obtained for plasma samples and the stan-

dard curve was used to accurately quantify the concentration of tempol in the plasma sample (30).

Statistics

Quantitative results were analyzed with a one-way ANOVA using GraphPad Prism software (GraphPad Software, La Jolla, CA). Results are shown as mean ± SEM. A *p* value of <0.05 was considered statistically significant.

Results

Aortic coarctation model

We have previously developed and characterized an *in vivo* model of acute LO WSS by a mouse aortic coarctation (38). A representative WSS map is presented in Figure 1. The region upstream from the coarctation shows high magnitude WSS
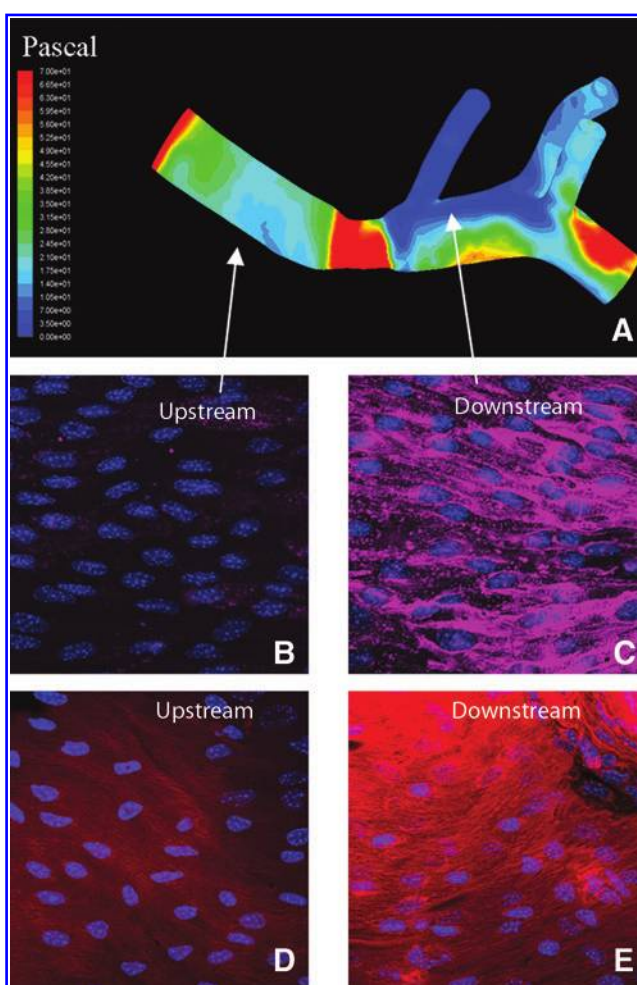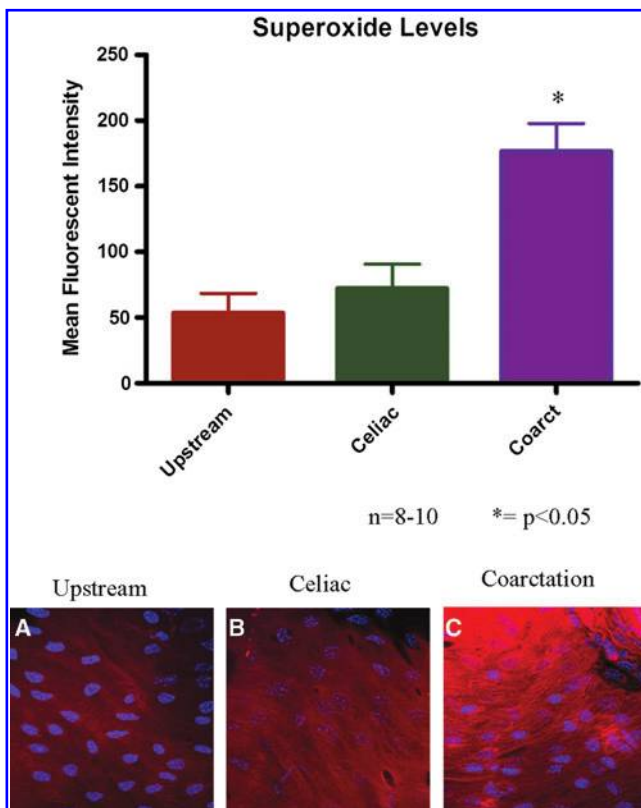

FIG. 1. The *upper panel* shows a representative WSS Map from an aorta with a coarctation. **(A)** There is low magnitude oscillatory WSS in the downstream region and high unidirectional WSS in the upstream region. The *lower images* show representative confocal images (63x) from *en face* mounted aortas stained for either VCAM-1 **(B** and **C)** or superoxide **(D** and **E).** The images on the *left* **(B** and **D)** were taken from the upstream region while the images on the *right* **(C** and **E)** were taken from the downstream region. (To see this illustration in color the reader is referred to the web version of this article at www.liebertonline.com/ars).

while the downstream region shows low magnitude WSS. As reported previously, flow is unidirectional in the upstream region and oscillatory in the downstream region. In the comparable downstream region of noncoarctation aortas, WSS is high and unidirectional, though more heterogeneity exists, particularly near the branch sites. Representative confocal images from the upstream and downstream regions show increased VCAM-1 and superoxide staining in the downstream region as compared to the upstream region (Figs. 1B–1E). This is a novel *in vivo* model of acutely disturbed flow, which can be used to investigate molecular mechanisms involved in the mechanotransduction of LO WSS.

Superoxide levels in response to LO WSS

Superoxide levels were quantitatively measured in the endothelium of mice using a novel hydrocyanine dye (Fig. 2). Low basal levels of superoxide were observed in the upstream region of the coarctation, corresponding to high magnitude unidirectional flow. In the celiac region of control, noncoarctation animals, where WSS is similarly high and unidirectional, there was no significant change in superoxide levels when compared to the upstream region. Animals with a co-
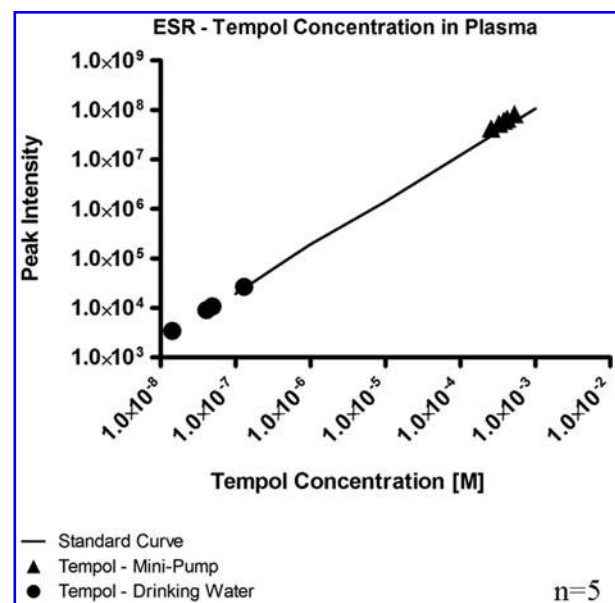
arctation experienced a region of low magnitude oscillatory WSS downstream from the coarctation. In this downstream region, superoxide levels were increased nearly four-fold in comparison to the two control groups.

Specificity and background noise have been limiting factors in previous attempts to measure superoxide in the endothelium. We administered tempol, an SOD mimetic that scavenges superoxide, to demonstrate the specificity of the hydrocyanine dye. We used electron spin resonance (ESR) to determine the plasma levels of tempol after administration in the drinking water. Tempol administration in drinking water resulted in a mean plasma tempol concentration of 46.9 ± 22.6 nM (Fig. 3). Superoxide levels in these mice were the same in the upstream and downstream regions, as compared to the respective regions in control mice. We then increased the plasma levels of tempol by intravenous administration by osmotic mini-pump. This dose produced a mean tempol plasma concentration of $383.1 \pm 45.3 \,\mu M$, significantly higher than the plasma concentration after drinking water administration. Superoxide levels in mice in the mini-pump group were significantly attenuated in comparison to the respective regions in control mice (Fig. 4, $p < 0.05$); levels in the upstream region were reduced by 79% while levels in the downstream region were reduced by 63%. Downstream superoxide levels after treatment of tempol by mini-pump were comparable to the upstream superoxide levels in the control animals.

Superoxide as a shear-sensitive signaling molecule

Tempol-treated mice (drinking water and mini-osmotic pump) were used with our coarctation model to investigate the role of superoxide as a mediator of VCAM-1 expression in response to changes in WSS. In control mice with no tempol treatment, VCAM-1 expression was relatively low in the
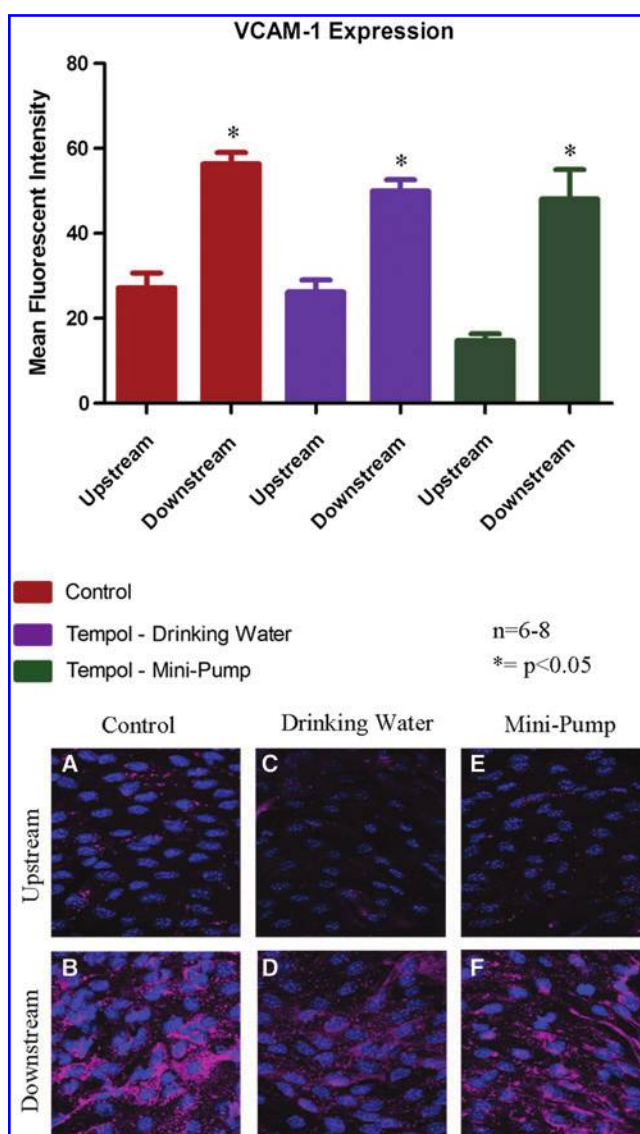

FIG. 2. Superoxide levels were measured using hydro-Cy3. Superoxide levels significantly increased in the downstream region as compared to the control regions. The *right images* show representative confocal images from *en face* mounted aortas: **(A)** is from the upstream region, **(B)** is from the downstream region from a control, non-coarctation aorta, **(C)** is from the downstream region from a coarctation aorta. $N = 8$–10; *$p < 0.05$. (To see this illustration in color the reader is referred to the web version of this article at www.liebertonline.com/ars).

FIG. 3. ESR was used to measure plasma concentrations of tempol. Tempol administration through drinking water produced plasma tempol concentrations that were significantly lower than the plasma concentrations when tempol was administered by osmotic mini-pump; $n = 5$.
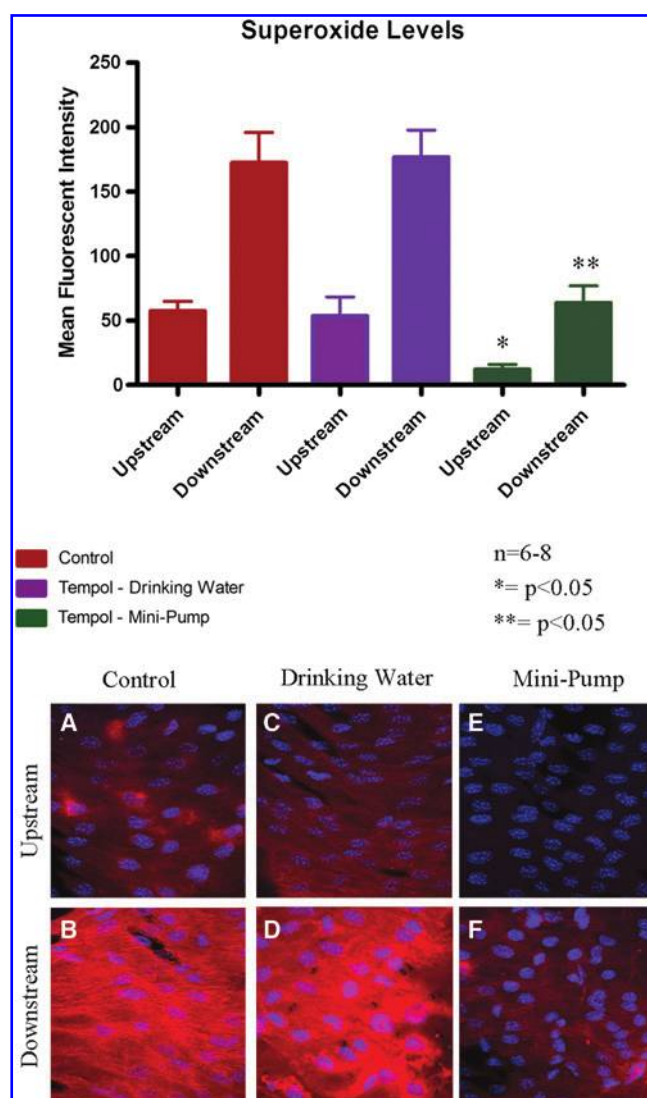
FIG. 4. Superoxide levels were measured in tempol-treated mice. Tempol treatment administered through the drinking water produced no change in superoxide levels in either the upstream or downstream region when compared to the control. Tempol treatment by osmotic mini-pump significantly attenuated the superoxide levels in the upstream and downstream regions in comparison to the control. Representative confocal images from *en face* mounted aortas are presented on the *bottom of the figure*: **A**, **C**, and **E** are from the upstream region; **B**, **D**, and **F** are from the downstream region from a coarctation aorta; **A** and **B** are from control mice; **C** and **D**.are from mice treated with tempol administered by drinking water; **E** and **F** are from mice treated with tempol administered by mini-pump. $N = 6$–8, *$p < 0.05$ comparing upstream regions of the three group, **$p < 0.05$ comparing downstream regions of the three groups. (To see this illustration in color the reader is referred to the web version of this article at www.liebertonline.com/ars).


FIG. 5. VCAM-1 expression was measured in mice treated with tempol. Tempol treatment, regardless of mode of administration, had no effect on VCAM-1 expression in either the upstream region or the downstream region when compared to the control. Representative confocal images from *en face* mounted aortas stained for VCAM-1 are presented. **A**, **C**, and **E** are from the upstream region; **B**, **D**, and **F** are from the downstream region from a coarctation aorta; **A** and **B** are from control mice; C and D.are from mice treated with tempol administered by drinking water; **E** and **F** are from mice treated with tempol administered by mini-pump. $N = 6$–8, *$p < 0.05$ comparing upstream region to downstream region. (To see this illustration in color the reader is referred to the web version of this article at www.liebertonline.com/ars).

upstream region, where cells are exposed to high magnitude unidirectional WSS (Fig. 5). VCAM-1 expression significantly increased in the downstream region that was acutely exposed to LO WSS ($p < 0.05$). Mice treated with tempol administered through drinking water showed the same VCAM-1 expression in both the upstream and downstream regions as compared to

the respective regions in the control, non-tempol-treated mice. Similarly, mice treated with tempol administered intravenously by mini-pump, showed no significant change in VCAM-1 expression in either the upstream or downstream region as compared to control, non-tempol-treated mice ($p < 0.05$). The tempol dose achieved by intravenous infusion was enough to attenuate the endothelial superoxide levels, but had no effect on vascular VCAM-1 expression.

Contribution of NADPH oxidase

The coarctation model was performed on p47 phox ko mice to investigate the contribution of NADPH oxidase to shear-dependent endothelial expression of both superoxide and VCAM-1. There was no significant difference in superoxide levels in the upstream region between the p47 phox ko mice and the control mice (Fig. 6). The superoxide levels increased significantly in the downstream region in both groups of mice, with no significant change in the downstream superoxide levels between the p47 phox ko mice and the control. VCAM-1 expression followed a similar pattern; expression upstream was comparable between control and p47 phox ko mice, while expression downstream increased significantly in both groups with no significant difference between the p47 phox ko mice and the control (Fig. 7).
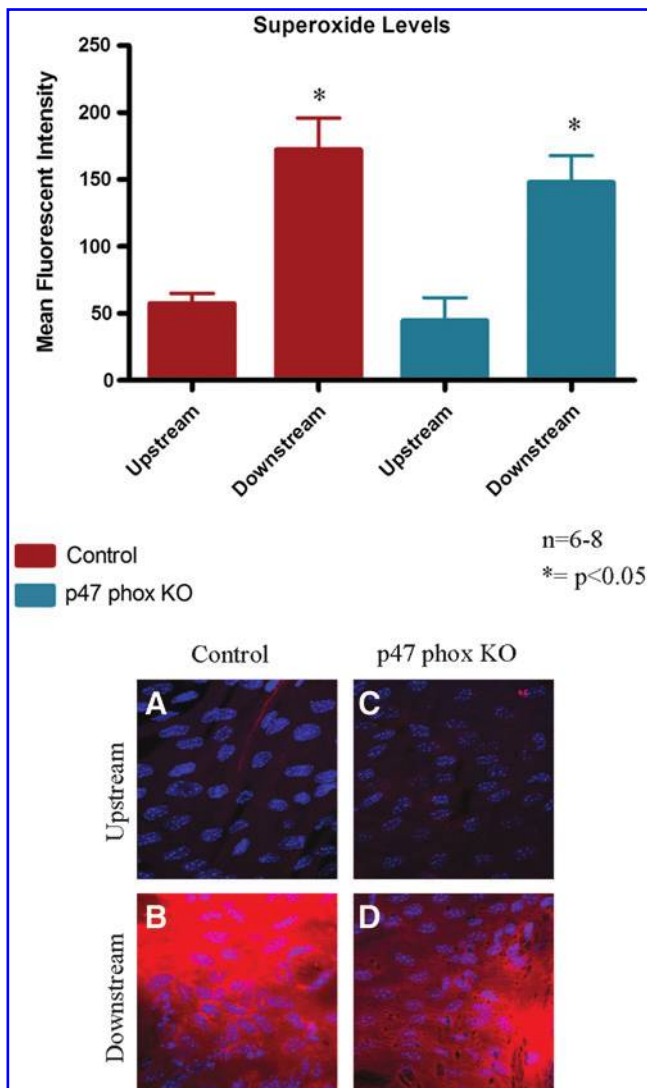

FIG. 6. Superoxide levels were measured in p47 phox ko mice. P47 phox ko mice showed superoxide levels that were comparable to the control in both the upstream and downstream regions. Representative confocal images from *en face* mounted aortas are presented. $N = 6–8$, *$p < 0.05$ comparing upstream region to downstream region. (To see this illustration in color the reader is referred to the web version of this article at www.liebertonline.com/ars).
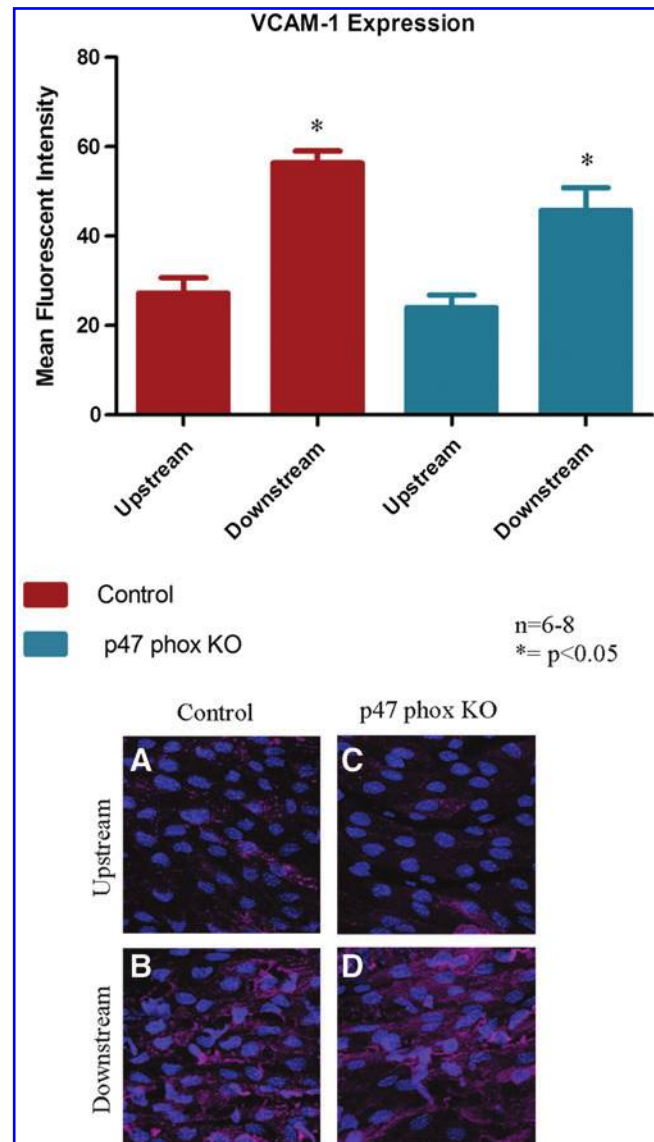
FIG. 7. VCAM-1 expression was measured in p47 phox ko mice. There was no significant change in VCAM-1 expression in either the upstream or downstream regions when compared with the control. Representative confocal images are shown: **A** and **C** are from the upstream region; **B** and **D** are from the downstream region; **A** and **B** are from control mice while **C** and **D** are from p47 phox ko mice. $N = 6–8$, *$p < 0.05$ comparing upstream region to downstream region. (To see this illustration in color the reader is referred to the web version of this article at www.liebertonline.com/ars).

Contribution of hydrogen peroxide

We used two complimentary murine models of decreased hydrogen peroxide levels to further investigate the potential contribution of ROS to shear-dependent VCAM-1 expression. Transgenic mice overexpressing catalase in the vascular wall showed a trend for attenuated VCAM-1 expression in the upstream region compared with the control. However, VCAM-1 expression in the downstream region of the catalase overexpressing mice increased significantly compared with the upstream region, though expression was not significantly different from that of the control (Fig. 8). Similarly, ebselen-
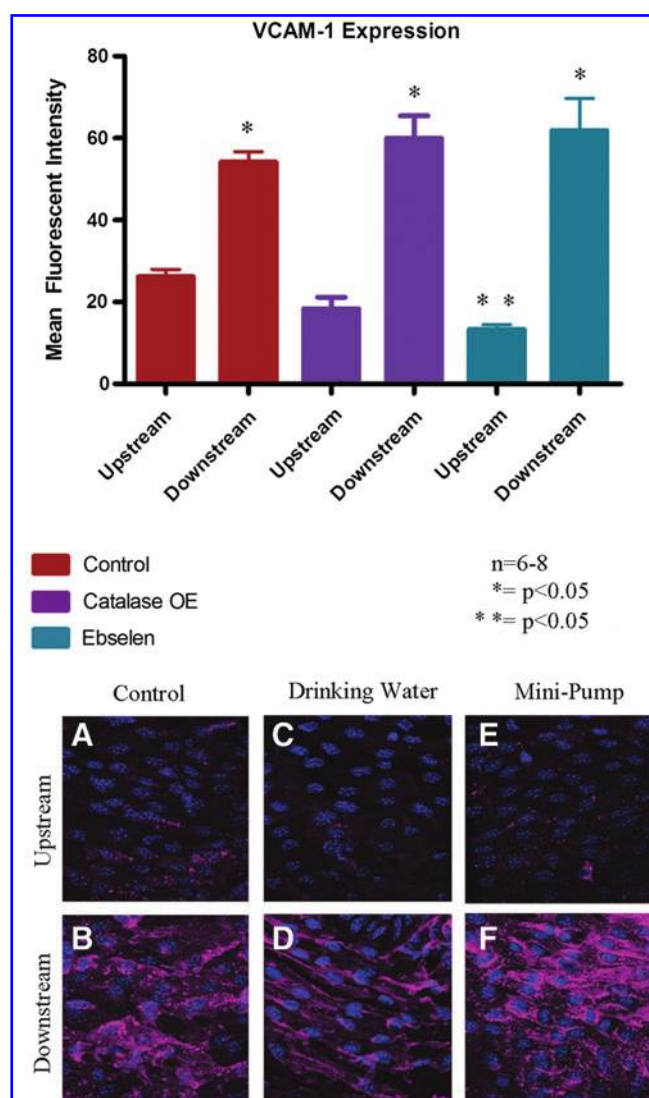
FIG. 8. VCAM-1 expression was measured in catalase-overexpressing mice and ebselen-treated mice. There was no significant change in VCAM-1 expression in the upstream or downstream regions from either treatment group when compared with the control. Representative confocal images from *en face* mounted aortas stained for VCAM-1 are presented. **A**, **C**, and **E** are from the upstream region; **B**, **D**, and **F** are from the downstream region from a coarctation aorta; **A** and **B** are from control mice; **C** and **D** are from catalase-overexpressing mice; **E** and **F** are from mice treated with ebselen. $N = 6$–8, *$p < 0.05$ comparing upstream region to downstream region; **$p < 0.05$ comparing upstream region of control to upstream region ebselen treated. (To see this illustration in color the reader is referred to the web version of this article at www.liebertonline.com/ars).

treated mice showed attenuated VCAM-1 expression in the upstream region compared to the control ($P < 0.05$), yet expression in the downstream region increased to a level comparable to that of the control.

Discussion

Models of disturbed flow in small animals provide a new platform to investigate *in vivo* the molecular mechanisms in-

volved in flow-mediated atherogenesis. In this study, we used a novel aortic coarctation model that acutely produces regions of LO WSS. We combined this model with a novel superoxide sensitive dye, hydro-cyanine 3, to look at endothelial superoxide levels in response to acute changes in flow. We then used pharmacologic treatments and genetically modified animals to investigate the role of ROS in mediating shear dependent signaling.

Dihydroethidium (DHE) is the current gold standard for superoxide detection in tissue; however, DHE requires complex purification prior to use, it has a short half life, and it is light sensitive. Superoxide is a highly unstable and short-lived molecule that rapidly reacts with other cellular molecules, such as superoxide dismutase (SOD) and nitric oxide (NO). It is challenging to employ this unstable dye to detect an unstable molecule, particularly when trying to image small localized regions in the endothelium. Additionally, DHE has not been used for histology of whole tissue preparations, specifically *en face* mounted tissue. Previous attempts by our group to measure superoxide levels using DHE for *en face* histology have proved unsuccessful (data not shown). One reason is that whole tissue preparations require the tissue, and thus the dye, to be exposed to light during mounting, which is not optimal for DHE use. Therefore, we used the hydro-cyaninne 3 dye, which is more stable than DHE, to measure regional tissue levels of endothelial superoxide.

In this study, we present a novel use of the hydro-cyanine 3 dye to quantitatively measure endothelial superoxide levels in regions of varying WSS. We found that superoxide levels increase significantly in regions of LO WSS as compared to regions of high unidirectional WSS, similar to published data from *in vitro* studies (15, 16, 21, 32, 33). Previous reports have demonstrated the specificity of the dye *in vitro* by using tempol as a means to scavenge superoxide molecule (19). Similarly, we found that hydro-Cy3 measurements of endothelial superoxide levels could in fact be attenuated by treatment with tempol; however, it was necessary for the mode and dose of delivery to increase the plasma concentration to sufficient levels.

We measured plasma concentrations of tempol and endothelial superoxide levels from animals treated with tempol administered by either intravenous mini-pump or drinking water. Previously, an *in vitro* dose response study showed that administration of tempol at a concentration on the order of 1 mM inhibited 75% of superoxide production when stimulated with angiotensin II, while tempol concentrations on the order of 100 nM inhibited 10% of superoxide production (22). Though the stimulus in our paper was different (WSS instead of angiotensin II) the findings were similar. Tempol treatment administered IV by mini-pump produced plasma concentrations on the order of 1 mM and was able to attenuate superoxide levels. However, tempol treatment administered in the drinking water produced plasma levels on the order of 100 nM and had no significant effect on observed endothelial superoxide production. In future studies, it should therefore be taken into account that although tempol treatment in the drinking water has been shown to produce systemic effects, it does not sufficiently increase plasma tempol levels to a concentration where endothelial superoxide production is significantly inhibited.

Though tempol treatment was able to attenuate endothelial superoxide levels in the upstream and downstream regions as

compared to the control, it is important to note that there was still a significant increase in superoxide levels in the downstream region as compared to the upstream region. However, the level of superoxide present was equivalent to the baseline levels seen in control animals.

We quantitatively measured VCAM-1 using quantum dot based *en face* immunohistochemistry. This methodology specifically quantifies endothelial protein expression, since the quantum dot-antibody conjugates do not penetrate into the media of the aorta (12). As was previously reported, we found that VCAM-1 levels increased significantly in the downstream region as compared with the upstream region. Tempol treatment, regardless of mode of administration, had no effect on the upstream or downstream expression of VCAM-1 as compared to the control. These data suggest that superoxide does not mediate shear stress-mediated changes in endothelial VCAM-1 expression in the aorta.

Since tempol treatment suggests that there may be differences between *in vivo* and *in vitro* signaling pathways, we wanted to investigate the mechanisms of shear-dependent superoxide formation by looking at the *in vivo* contribution of the NADPH oxidase subunit, p47 phox. Previous studies found that p47 phox had a functional role in shear-dependent superoxide formation and subsequent inflammatory protein expression (16, 25, 33, 34). Our study, however, found that in p47 phox ko mice, superoxide levels increased significantly in the downstream region as compared to the upstream region and neither region was significantly different from that of the control. We specifically show this response in the endothelium, whereas previous *in vivo* studies may have been measuring superoxide produced by additional cell types, such as macrophages. Additionally, VCAM-1 expression in p47 phox ko mice was comparable in both regions to the expression in control mice. These results show that *in vivo* endothelial production of superoxide in response to LO WSS is not p47 phox dependent and suggest the presence of compensatory or parallel pathways *in vivo*.

P47 phox ko mice have some clear limitations with regards to analysis of the entire NOX family. The p47 phox subunit is not present in all NOX family members, of particular note is NOX 4. NOX 4, in fact, has been shown to be upregulated in p47 phox ko mice (D. Sorescu, Emory University School of Medicine, personal communication). This compensatory mechanism could account for the lack of change in superoxide levels and may even produce an additional increase in other oxidants, primarily hydrogen peroxide. Additionally, there could be parallel pathways acting to increase VCAM-1 expression. Studies have suggested that other mechanosensitive mechanisms, such as Flk1 activation, may activate the transcription factor NF-κB, thereby increasing VCAM-1 expression (26, 36). Similarly, *in vivo* findings in the lesser curvature of the porcine aortic arch found an upregulation of inflammatory markers in the NF-κB pathway along with a paradoxical increase in antioxidative gene expression, again suggesting a parallel pathway (27). Alternatively, other transcription factors, such as AP-1, may be involved in endothelial mechanotransduction (13, 20). Since *in vitro* studies had shown that p47 phox ko cells attenuated superoxide production in response to LO WSS, we chose this model as our focus (33).

Alternative methods for investigating the NADPH oxidase family do exist, primarily the use of the inhibitors apocynin or DPI, yet these have their own limitations. Apocynin has been shown to stimulate ROS production in nonphagocytic cells (39). In preliminary studies by our group, we saw increased basal VCAM-1 levels throughout the vasculature with apocynin use and thus chose not to pursue this path (data not shown). DPI, on the other hand, inhibits all flavin-containing enzymes, including eNOS (1). eNOS is responsive to WSS and when uncoupled is believed to play a role in endothelial superoxide generation (14). DPI is therefore not an ideal treatment when trying to isolate molecular mechanisms involving the NOX family from other oxidant-producing enzymes. Recent reviews of these treatments have discussed the lack of specificity of both reagents as well as the ability to produce oxidative stress and therefore recommend use of other means to investigate the NOX family (1).

Although compensatory and parallel mechanisms may be directly affecting superoxide levels in this model, it is also feasible that these pathways may also affect other oxidants. Of particular interest is hydrogen peroxide. NOX family members, specifically Nox-4, can directly produce hydrogen peroxide and SOD scavenges superoxide producing hydrogen peroxide (9). We therefore wanted to investigate whether decreasing hydrogen peroxide levels might inhibit inflammatory protein expression. We found that VCAM-1 expression was not attenuated in the LO WSS region in either catalase-overexpressing mice or mice treated with ebselen. A limitation of these experiments is the lack of accurate methods for the measurement of hydrogen peroxide, therefore we cannot confirm the efficacy of the treatments. Hydrogen peroxide is challenging to measure *in vivo* and more challenging to measure specifically in the endothelium. The dye DCFDA is sometimes used to measure hydrogen peroxide levels; however, recent reviews have shown evidence for the instability of the molecule (8).

These results suggest the presence of parallel or compensatory pathways in shear-dependent oxidative stress and inflammatory protein expression *in vivo*. The techniques in this study are low throughput and we therefore focused on oxidants that had been shown to be responsive to LO WSS in prior studies. Other inflammatory and oxidative markers of interest for future studies may include ICAM-1, BMP-4, NF-κB, eNOS, xanthine oxidase, and peroxynitrite, among others. A recent *in vivo* study gives our group particular interest in investigating eNOS and the angiotensin I receptor(AT$_1$R). It was shown that AT$_1$R expression increased in atheroprone regions that could be blocked in eNOS-overexpressing mice (29). This implicates another pathway by which LO WSS might stimulate an endothelial inflammatory response.

As a result of this study, we conclude that shear-dependent oxidative stress *in vivo* is a complex process. Superoxide is acutely responsive to LO WSS, as is VCAM-1. In this model, VCAM-1 expression does not appear to be dependent on superoxide levels. Furthermore, compensatory mechanisms or parallel pathways appear to exist *in vivo* in the production of superoxide, and this pathway is not solely dependent on p47 phox. Though *in vitro* studies can provide valuable insight into molecular mechanisms involved in atherogenesis, it is still important to investigate these molecular mechanisms *in vivo* for greater understanding of the development of atherosclerotic plaques. Finally, we show that models of decreased hydrogen peroxide do not inhibit shear-dependent VCAM-1 expression, suggesting that hydrogen peroxide is

not crucial in VCAM-1 upregulation as a result of LO WSS. Mechanically-induced oxidative stress is clearly a complex mechanism and further research is required to determine the many pathways that are involved.

Acknowledgments

Author Disclosure Statement

W. Robert Taylor, Niren Murthy, and Kousik Kundu have an equity interest in Reactive Diagnostics, Inc.

References

1. Aldieri E, Riganti C, Polimeni M, Gazzano E, Lussiana C, Campia I, and Ghigo D. Classical inhibitors of NOX NAD(P)H oxidases are not specific. *Curr Drug Metab* 9: 686–696, 2008.

2. Amirbekian S, Long RC, Jr., Consolini MA, Suo J, Willett NJ, Fielden SW, Giddens DP, Taylor WR, and Oshinski JN. *In vivo* assessment of blood flow patterns in abdominal aorta of mice with MRI: Implications for AAA localization. *Am J Physiol Heart Circ Physiol* 297: H1290–1295, 2009.

3. Basta G, Lazzerini G, Del Turco S, Ratto GM, Schmidt AM, and De Caterina R. At least 2 distinct pathways generating reactive oxygen species mediate vascular cell adhesion molecule-1 induction by advanced glycation end products. *Arterioscler Thromb Vasc Biol* 25: 1401–1407, 2005.

4. Brooks AR, Lelkes PI, and Rubanyi GM. Gene expression profiling of human aortic endothelial cells exposed to disturbed flow and steady laminar flow. *Physiol Genomics* 9: 27–41, 2002.

5. Chappell DC, Varner SE, Nerem RM, Medford RM, and Alexander RW. Oscillatory shear stress stimulates adhesion molecule expression in cultured human endothelium. *Circ Res* 82: 532–539, 1998.

6. Cheng C, Tempel D, van Haperen R, van der Baan A, Grosveld F, Daemen MJ, Krams R, and de Crom R. Atherosclerotic lesion size and vulnerability are determined by patterns of fluid shear stress. *Circulation* 113: 2744–2753, 2006.

7. Cybulsky MI, Iiyama K, Li H, Zhu S, Chen M, Iiyama M, Davis V, Gutierrez-Ramos JC, Connelly PW, and Milstone DS. A major role for VCAM-1, but not ICAM-1, in early atherosclerosis. *J Clin Invest* 107: 1255–1262, 2001.

8. Dikalov S, Griendling KK, and Harrison DG. Measurement of reactive oxygen species in cardiovascular studies. *Hypertension* 49: 717–727, 2007.

9. Dikalov SI, Dikalova AE, Bikineyeva AT, Schmidt HH, Harrison DG, and Griendling KK. Distinct roles of Nox1 and Nox4 in basal and angiotensin II-stimulated superoxide and hydrogen peroxide production. *Free Radic Biol Med* 45: 1340–1351, 2008.

10. Dikalova A, Clempus R, Lassegue B, Cheng G, McCoy J, Dikalov S, San Martin A, Lyle A, Weber DS, Weiss D, Taylor WR, Schmidt HH, Owens GK, Lambeth JD, and Griendling KK. Nox1 overexpression potentiates angiotensin II-induced hypertension and vascular smooth muscle hypertrophy in transgenic mice. *Circulation* 112: 2668–2676, 2005.

11. Duvall CL, Taylor WR, Weiss D, and Guldberg RE. Quantitative microcomputed tomography analysis of collateral vessel development after ischemic injury. *Am J Physiol Heart Circ Physiol* 287: H302–310, 2004.

12. Ferrara DE, Weiss D, Carnell PH, Vito RP, Vega D, Gao X, Nie S, and Taylor WR. Quantitative 3D fluorescence technique for the analysis of en face preparations of arterial walls using quantum dot nanocrystals and two-photon excitation laser scanning microscopy. *Am J Physiol Regul Integr Comp Physiol* 290: R114–123, 2006.

13. Fledderus JO, van Thienen JV, Boon RA, Dekker RJ, Rohlena J, Volger OL, Bijnens AP, Daemen MJ, Kuiper J, van Berkel TJ, Pannekoek H, and Horrevoets AJ. Prolonged shear stress and KLF2 suppress constitutive proinflammatory transcription through inhibition of ATF2. *Blood* 109: 4249–4257, 2007.

14. Harrison DG, Widder J, Grumbach I, Chen W, Weber M, and Searles C. Endothelial mechanotransduction, nitric oxide and vascular inflammation. *J Intern Med* 259: 351–363, 2006.

15. Hwang J, Ing MH, Salazar A, Lassegue B, Griendling K, Navab M, Sevanian A, and Hsiai TK. Pulsatile versus oscillatory shear stress regulates NADPH oxidase subunit expression: Implication for native LDL oxidation. *Circ Res* 93: 1225–1232, 2003.

16. Hwang J, Saha A, Boo YC, Sorescu GP, McNally JS, Holland SM, Dikalov S, Giddens DP, Griendling KK, Harrison DG, and Jo H. Oscillatory shear stress stimulates endothelial production of O2- from p47phox-dependent NAD(P)H oxidases, leading to monocyte adhesion. *J Biol Chem* 278: 47291–47298, 2003.

17. Jongstra–Bilen J, Haidari M, Zhu SN, Chen M, Guha D, and Cybulsky MI. Low-grade chronic inflammation in regions of the normal mouse arterial intima predisposed to atherosclerosis. *J Exp Med* 203: 2073–2083, 2006.

18. Kawada N, Imai E, Karber A, Welch WJ, and Wilcox CS. A mouse model of angiotensin II slow pressor response: Role of oxidative stress. *J Am Soc Nephrol* 13: 2860–2868, 2002.

19. Kundu K, Knight SF, Willett N, Lee S, Taylor WR, and Murthy N. Hydrocyanines: A class of fluorescent sensors that can image reactive oxygen species in cell culture, tissue, and *in vivo*. *Angew Chem Int Ed Engl* 48: 299–303, 2009.

20. Lan Q, Mercurius KO, and Davies PF. Stimulation of transcription factors NF kappa B and AP1 in endothelial cells subjected to shear stress. *Biochem Biophys Res Commun* 201: 950–956, 1994.

21. Li JM and Shah AM. Endothelial cell superoxide generation: Regulation and relevance for cardiovascular pathophysiology. *Am J Physiol Regul Integr Comp Physiol* 287: R1014–1030, 2004.

22. Luo Z, Chen Y, Chen S, Welch WJ, Andresen BT, Jose PA, and Wilcox CS. Comparison of inhibitors of superoxide generation in vascular smooth muscle cells. *Br J Pharmacol* 157: 935–943, 2009.

23. Mohan S, Hamuro M, Sorescu GP, Koyoma K, Sprague EA, Jo H, Valente AJ, Prihoda TJ, and Natarajan M. IkappaBalpha-dependent regulation of low-shear flow-induced NF-kappa B activity: Role of nitric oxide. *Am J Physiol Cell Physiol* 284: C1039–1047, 2003.

24. Mohan S, Mohan N, Valente AJ, and Sprague EA. Regulation of low shear flow-induced HAEC VCAM-1 expression and monocyte adhesion. *Am J Physiol* 276: C1100–1107, 1999.

25. Nam D, Ni CW, Rezvan A, Suo J, Budzyn K, Llanos A, Harrison D, Giddens D, and Jo H. Partial carotid ligation is a

model of acutely induced disturbed flow, leading to rapid endothelial dysfunction and atherosclerosis. *Am J Physiol Heart Circ Physiol* 297: H1535–1543, 2009.

26. Orr AW, Sanders JM, Bevard M, Coleman E, Sarembock IJ, and Schwartz MA. The subendothelial extracellular matrix modulates NF-kappaB activation by flow: A potential role in atherosclerosis. *J Cell Biol* 169: 191–202, 2005.

27. Passerini AG, Polacek DC, Shi C, Francesco NM, Manduchi E, Grant GR, Pritchard WF, Powell S, Chang GY, Stoeckert CJ, Jr., and Davies PF. Coexisting proinflammatory and antioxidative endothelial transcription profiles in a disturbed flow region of the adult porcine aorta. *Proc Natl Acad Sci USA* 101: 2482–2487, 2004.

28. Pueyo ME, Gonzalez W, Nicoletti A, Savoie F, Arnal JF, and Michel JB. Angiotensin II stimulates endothelial vascular cell adhesion molecule-1 via nuclear factor-kappaB activation induced by intracellular oxidative stress. *Arterioscler Thromb Vasc Biol* 20: 645–651, 2000.

29. Ramkhelawon B, Vilar J, Rivas D, Mees B, de Crom R, Tedgui A, and Lehoux S. Shear stress regulates angiotensin type 1 receptor expression in endothelial cells. *Circ Res* 105: 869–875, 2009.

30. Saito K, Takeshita K, Ueda J, and Ozawa T. Two reaction sites of a spin label, TEMPOL (4-hydroxy-2,2,6,6-tetra-methylpiperidine-N-oxyl), with hydroxyl radical. *J Pharm Sci* 92: 275–280, 2003.

31. San Martin A, Du P, Dikalova A, Lassegue B, Aleman M, Gongora MC, Brown K, Joseph G, Harrison DG, Taylor WR, Jo H, and Griendling KK. Reactive oxygen species-selective regulation of aortic inflammatory gene expression in Type 2 diabetes. *Am J Physiol Heart Circ Physiol* 292: H2073–2082, 2007.

32. Sorescu D, Weiss D, Lassegue B, Clempus RE, Szocs K, Sorescu GP, Valppu L, Quinn MT, Lambeth JD, Vega JD, Taylor WR, and Griendling KK. Superoxide production and expression of nox family proteins in human atherosclerosis. *Circulation* 105: 1429–1435, 2002.

33. Sorescu GP, Song H, Tressel SL, Hwang J, Dikalov S, Smith DA, Boyd NL, Platt MO, Lassegue B, Griendling KK, and Jo H. Bone morphogenic protein 4 produced in endothelial cells by oscillatory shear stress induces monocyte adhesion by stimulating reactive oxygen species production from a nox1-based NADPH oxidase. *Circ Res* 95: 773–779, 2004.

34. Sorescu GP, Sykes M, Weiss D, Platt MO, Saha A, Hwang J, Boyd N, Boo YC, Vega JD, Taylor WR, and Jo H. Bone morphogenic protein 4 produced in endothelial cells by oscillatory shear stress stimulates an inflammatory response. *J Biol Chem* 278: 31128–31135, 2003.

35. Suo J, Ferrara DE, Sorescu D, Guldberg RE, Taylor WR, and Giddens DP. Hemodynamic shear stresses in mouse aortas: Implications for atherogenesis. *Arterioscler Thromb Vasc Biol* 27: 346–351, 2007.

36. Wang Y, Flores L, Lu S, Miao H, Li YS, and Chien S. Shear stress regulates the Flk-1/Cbl/PI3K/NF-kappaB pathway via actin and tyrosine kinases. *Cell Mol Bioeng* 2: 341–350, 2009.

37. Wilcox CS and Pearlman A. Chemistry and antihypertensive effects of tempol and other nitroxides. *Pharmacol Rev* 60: 418–469, 2008.

38. Willett NJ, Long RC Jr, Maiellaro-Rafferty K, Sutliff RL, Shafer R, Oshinski JN, Giddens DP, Guldberg RE, and Taylor WR. An in vivo murine model of low-magnitude oscillatory wall shear stress to address the molecular mechanisms of mechanotransduction. *Arterioscler Thromb Vasc Biol* 30: 2099–2102, 2010.

39. Ximenes VF, Kanegae MP, Rissato SR, and Galhiane MS. The oxidation of apocynin catalyzed by myeloperoxidase: Proposal for NADPH oxidase inhibition. *Arch Biochem Biophys* 457: 134–141, 2007.

Address correspondence to:
Dr. W. Robert Taylor
Division of Cardiology
Emory University School of Medicine
1639 Pierce Drive, Suite 319 WMB
Atlanta, GA, 30322

E-mail: wtaylor@emory.edu

Abbreviations Used

AT$_1$R = angiotensin 1 receptor
DPI = diphenyleneiodonium
ko = knockout
LO WSS = low magnitude oscillatory wall shear stress
ROS = reactive oxygen species
VCAM = vascular cell adhesion molecule

This article has been cited by:

1. Nathan T. Jenkins, Jeffrey S. Martin, M. Harold Laughlin, Jaume Padilla. 2012. Exercise-Induced Signals for Vascular Endothelial Adaptations: Implications for Cardiovascular Disease. *Current Cardiovascular Risk Reports* . [CrossRef]
2. Noriko Noguchi , Hanjoong Jo . Redox Going with Vascular Shear Stress. *Antioxidants & Redox Signaling*, ahead of print. [Abstract] [Full Text HTML] [Full Text PDF] [Full Text PDF with Links]